

Self-Assembly of Glycine on Cu (001): the Tales of Polarity and Temperature

Jing Xu,¹ Zheshuai Lin,² Sheng Meng,³ Lifang Xu,^{3,*} and Enge Wang⁴

¹Department of Physics, Renmin University of China, Beijing 100872, China

²Technical Institute of Physics and Chemistry, Chinese Academy of Sciences, Beijing 100190, China

³Beijing National Laboratory for Condensed Matter Physics, Institute of Physics, Chinese Academy of Sciences, P.O. Box 603, Beijing 100190, China

⁴School of Physics, Peking University, Beijing 100871, China

(Dated: August 3, 2018)

Glycine on Cu(001) is used as an example to illustrate the critical role of molecular polarity and finite temperature effect in self-assembly of biomolecules at a metal surface. A unified picture for glycine self-assembly on Cu(001) is derived based on full polarity compensation considerations, implemented as a generic rule. Temperature plays a non-trivial role: the ground-state structure at 0 K is absent at room temperature, where intermolecular hydrogen bonding overweighs competing molecule-substrate interactions. The unique $p(2\times 4)$ structure from the rule is proved as the most stable one by *ab initio* molecular dynamics at room temperature, and its STM images and anisotropic free-electron-like dispersion are in excellent agreement with experiments. Moreover, the rich self-assembling patterns including the heterochiral and homochiral phases, and their interrelationships are entirely governed by the same mechanism.

PACS numbers: 81.16.Dn, 82.30.Rs, 68.43.Bc, 68.43.Hn

Self-assembly (SA) of molecules on a solid surface is particularly interesting for both fundamental research and potential applications in the mass fabrication of nanoscale devices [1–13]. This approach is a promising route to construct the functional systems with nanometre dimensions by autonomous ordering of molecules on atomically well-defined surfaces. The comprehensive understandings of the mechanisms controlling the SA phenomena can steer the SA and growth processes. Various molecular patterns have been observed in scanning tunneling microscopy (STM) for organic molecules on metal surfaces, e.g. self-assembled supermolecular clusters and chains on Au or Ag surfaces [3–6]; chiral metal-organic complexes on Cu(001) [14]; and a homomolecular two-dimensional honeycomb network at a Cu(111) surface [11]. These organic molecules are usually planar and rigid, and directly observable with STM. For biomolecules, however, due to their complicated structures and properties such as chirality, it is not possible to reach an atomic resolution in STM images, which generally appear as bright protrusions [12, 13]. For example, recent STM studies on glycine monolayer on Cu (001) displayed a blurred profile of molecules even at a temperature as low as 5 K [15]. Therefore, it is great desirable to investigate the basic molecular self-assembled structures beyond the STM results.

Glycine, the simplest amino acid comprising only an amino group (as the head) and a carboxyl group (as the tail), is one of most fundamental components for biomolecules. Among all amino acids glycine is the only one that does not have chirality. However, by adsorbing on Cu surfaces glycine deprotonates and changes to glycinate ion. Thus, the amino and carboxyl groups of glycinate are strongly positively and negatively polarized, respectively, upon surface adsorption, exhibit-

ing two different chiral configurations. Plenty of structural patterns including the $p(2\times 4)$ heterochiral phase, $c(2\times 4)$ homochiral phase, and mixed phases with different domain boundaries have been observed for glycine on Cu (001) [16]. To explain the stability of these various phases, Kanazawa et al. proposed a two-step mechanism, i.e., the $c(2\times 4)$ phase is stabilized by the formation of the $\langle 310 \rangle$ steps and the $p(2\times 4)$ structure by couplings of the molecular layer to Cu substrate [16]. This model ignores the roles of internal factors such as intermolecular hydrogen bonding (HB) between glycine molecules, which would be the intrinsic driving force for SA. Scanning tunneling spectroscopy (STS) further revealed anisotropic free-electron-like dispersions with electron effective mass differing by 10-fold along the [110] and $[\bar{1}10]$ directions, respectively [15]. Although with many tries [17, 18], building an atomistic model of glycine monolayer structure that is thermodynamically stable and reproducing this anisotropic electronic behavior has not been successful. The mechanism governing the self-assembly of glycine on Cu, which has been a long-term controversy, is still unclear.

In this work, we employed state-of-the-art first-principles calculations and extensive molecular dynamics (MD) simulations to investigate the SA structure of glycine on Cu(001). We discovered that the structure satisfying a complete polarity compensation reproduces well all known features observed in experiments including STM images and 10-fold anisotropic free-electron-like dispersion, and further predicted all possible homochiral and mixed phases for glycine on Cu(001). Our results indicate that molecular polarity and finite temperature play vital roles in determining the microscopic mechanisms for glycine SA on a metal substrate. The “ground-state structure” at 0 K is not stable at room temperature;

instead, thermal fluctuations weaken molecule-substrate interaction and favor intermolecular hydrogen bonds as determinative forces for glycine self-assembling on Cu surface, which is a unique intrinsic nature of self-assembly in this system.

Structure optimizations were performed within the framework of Density Functional Theory (DFT) using Vienna *ab initio* simulation package (VASP) [19, 20], in which projector-augmented wave pseudopotentials and generalized gradient approximation [21] were chosen. A plane wave basis set was used to expand the Kohn-Sham orbitals with a 400 eV kinetic energy cutoff. Glycine molecules were placed on a seven layer Cu(001) slab in a supercell with dimensions of $10.28\text{\AA} \times 10.28\text{\AA} \times 25\text{\AA}$. The Monkhorst-Pack scheme [22] was adopted for the Brillouin zone integration, and we have tested that a $4 \times 4 \times 1$ k -point mesh is sufficient to ensure a good convergence in the total energy differences. The atoms in the top four Cu layers were allowed to fully relax until the forces on them were all smaller than 0.03 eV/\AA . Energy convergence for the geometry optimization was better than 0.1 meV per atom. The time step in molecular dynamics simulations was chosen to be 0.5 fs . An equilibration process was first performed by slowly heating the systems from 0 K to 310 K . Then we examined thermal oscillations in atomic structure and free energy at 310 K in canonical ensemble using the Nosé algorithm.

Our first-principles calculations show that a single glycinate molecule and its enantiomeric isomer binds to the Cu (001) surface with an energy of 2.33 eV through one nitrogen atom and two oxygen atoms, all on top site of substrate Cu atoms, as schematically shown in Fig. 1(a). Then we examined the atomistic geometry of glycinate SA monolayers. Based on physical consideration and the characters of glycinate molecule, we found that the stable $p(2 \times 4)$ structures have the following features: First, due to strong attractions between the positively (amino head) and negatively polarized ends (carboxyl tail), glycinate molecules arrange themselves into a linear chain via head-to-tail HB along the $[110]$ direction; Second, these chains form an alternating anti-parallel pattern to eliminate the net polarity of the two-dimensional (2D) island; Third, the neighboring chains are also connected by weaker HB along the $[\bar{1}10]$ direction to make the monolayer structure an integral network. The above three polarity compensation reasons emphasize that the constructing glycinate SA arrangement is energetically favorable by maximizing intermolecular attractive interactions while removing the net polarity of 2D network on a surface. Under these restrictions, we *exclusively* reached a heterochiral $p(2 \times 4)$ structure of glycinate on Cu(001), as shown in Fig. 1(b). Glycinate molecules naturally alternate their chirality from one chain to the next, as required by the full polarity compensation, otherwise, less stable and isolated double-rows would form instead of the 2D monolayers as observed in experiment.

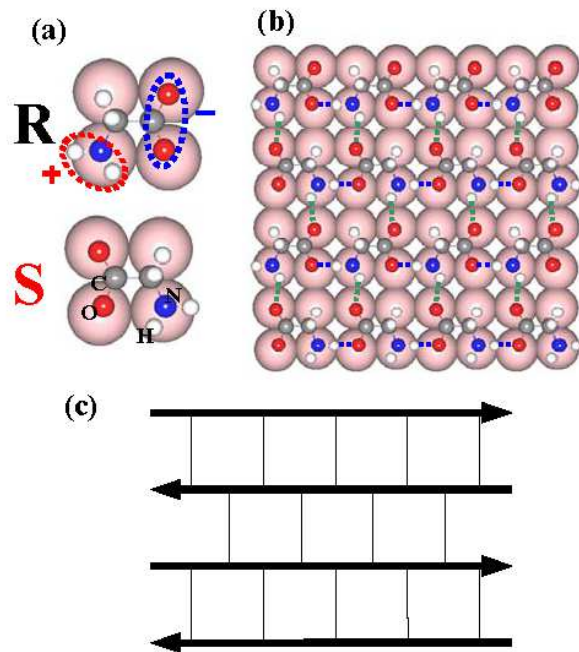


FIG. 1: (a) Adsorbed glycinate molecule (R) and its enantiomeric isomer (S). Two positive sites in amino group and two negative sites in carboxyl group are circled by red and blue dashed lines, respectively. (b) The anti-parallel molecular arrangement of a heterochiral $p(2 \times 4)$ structure. Each molecule interacts with four neighbors via HB. (c) Schematic plot of anti-parallel HB ladder-like network. Horizontal bold lines represent strong HB along $[110]$ and vertical thin lines weak HB along $[\bar{1}10]$. The arrows indicate the HB directions.

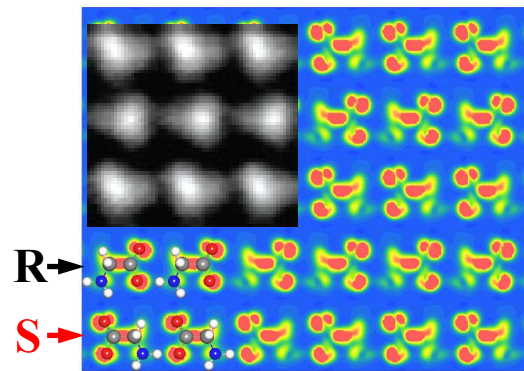
Geometry optimization shows that all O...H lengths in the HB along $[11]$ are 1.6 \AA with the binding energy of 210 meV (indicating a strong HB), whereas those along the $[\bar{1}10]$ direction are 2.0 \AA with the energy of 138 meV (weak HB) [23]. They are denoted in blue and green dashed lines in Fig. 1(b), respectively. This anti-parallel HB network is also schematically drawn in Fig. 1(c), to indicate the arrangement of molecular polarity. In this structure each glycinate acts as *two HB donors* and *two HB acceptors*, where all its polar sites are nicely saturated with HB [24]. This is consistent with the general understanding of H bonding interactions: namely, the selectivity, linearity, and saturation of H bonds.

Any structures proposed for glycine SA on Cu(001) would have to withstand stringent tests to reproduce properties measured experimentally; our structure model based on polarity compensation, shown in Fig. 1, satisfies these tests very well. To confirm it is indeed the one observed in experiment, we compare STM images, electronic band structure, structural phases, and energetics from both theory and experiment. Fig. 2(a) shows the simulated STM image for the $p(2 \times 4)$ phase, together with the measured image [15] in the inset for compari-

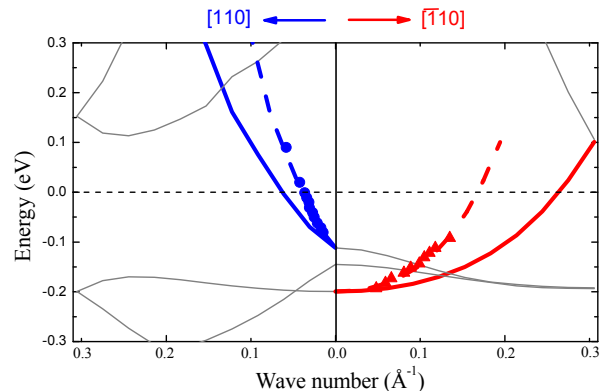
son. The STM image is calculated by integrating local states with energy <100 meV below the Fermi level within Tersoff-Hamann approximation [25]. It displays a pattern of triangular protrusions: triangles slightly tilted to the left are glycinate in S conformation, while those tilted to the right are in R conformation, forming an array of alternating anti-parallel rows. In experiment a pattern of blurred triangles with two orientations was observed, forming anti-parallel alternating rows along $[110]$, in a very similar manner to simulated images. Within each row the molecules are close to each other, indicating a stronger interaction within the rows; while there is a larger separation between the rows, suggesting weaker row-to-row interactions. These features are well reproduced and explained by our model.

More stringent test comes from the 10-fold difference in electron effective mass m_e^* for the free-electron-like dispersions along the $[110]$ and $[\bar{1}10]$ directions observed in STS [15]. Again this strong anisotropic behavior is obtained for our proposed $p(2\times 4)$ structure. We calculate the surface band structure of glycinate on a single Cu(001) layer, in order to remove the noisy background of bulk substrate. This approximation does not affect the anisotropic property because the removed Cu atoms are symmetric to the $[110]$ and $[\bar{1}10]$ directions. The results are shown in Fig. 2(b). There is only one band across Fermi surface for both $[110]$ and $[\bar{1}10]$ directions. The solid lines represent the calculated results, and the dashed lines are rescaled by multiplying a constant 2.46 for direct comparison with experimental data. Dashed curves perfectly match the experimental results, showing parabolic free-electron-like dispersions, as well as the 10-fold difference in the effective mass with respect to the $[110]$ and $[\bar{1}10]$ directions. The scaling constant is attributed to an enlarged effective mass m_e^* by using a single layer Cu in our approximation. Meanwhile, the Fermi energy is also shifted to include contributions from Cu layers underneath. Clearly, the anisotropy originates from different strengths of interactions between neighboring molecules in two directions, i.e., strong HB along the direction $[110]$ and weak HB along $[\bar{1}10]$, shown schematically in Fig. 1(c). Note that the weaker HBs are misaligned along $[\bar{1}10]$ which would significantly decrease the conductivity in this direction as well. Thus, different HB strengths together with their arrangements result in the 10-fold difference in the effective mass.

To interpret their STM observations, Kanazawa et al. adopted a structural model consisting of only head-to-tail alignments in the same direction, which is prevailing in literature for glycine SA on Cu(001) [12, 15, 16, 26]. For convenience of presentation, we name this structure the head-to-tail (HT) model. This model, however, does not consider the influence of polarity to side neighbors, not mention to the HB network. Thus, neither STM images nor free-electron-like dispersion in experiments were reproduced by the HT model. Indeed,



(a)



(b)

FIG. 2: (a) The calculated STM image for the $p(2\times 4)$ structure, the insert is experimental result from Ref. [15] for comparison. (b) Energy dispersion relations for the $[110]$ direction in blue and $[\bar{1}10]$ in red, respectively. Solid lines represent our calculated results and dashed lines are rescaled for comparison with experimental results from Ref. [15] (blue dots for $[110]$ and red triangles for $[\bar{1}10]$). The Fermi energy is indicated by horizontal dashed line.

first-principles calculation shows that the HT structure is 76 meV higher per molecule in energy than our structure for *free-standing* monolayers, indicating that our model is intrinsically more stable for SA than the HT model. In our $p(2\times 4)$ structure glycinate molecules are saturated with H bonds and all H bonds conform the ideality of H bonding interactions such as selectively and linearity, thus its free-standing structure is more stable than the unsaturated HT structure. The apparent $-\text{CH}\dots\text{O}$ hydrogen bonds with the length of 2.3 Å in the HT structure cannot be regarded as an ideal HB.

However, a complexity arises from the subtle balance between the intralayer molecule-molecule interactions and the molecule-substrate binding, which is a cen-

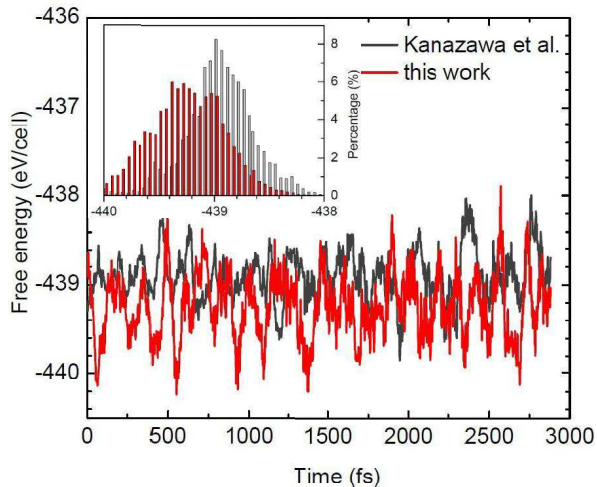


FIG. 3: Free energy fluctuations as a function of time in molecular dynamics simulations at 310 K for our structure and that adopted by Kanazawa et al. (Refs. [15,16]). The inset shows the distribution of free energies for the two cases.

tral theme in all SA processes. At 0 K, first principles calculations show that the HT model is lower in total energy by 140 meV per glycinate than the adsorption of our structure based on polarity compensation. That is, the HT model is the “ground state structure” for glycinate layer on Cu(001) at 0 K. Then why it is not observed in experiments, which shows very different STM/STS features as to those of the HT structure?

To solve this controversy, we performed *ab initio* MD simulations for both HT and our structure model at room temperature (RT) \sim 310 K. Both configurations are stable in trajectories lasting for 5 ps. However, we found the “ground state structure” at 0 K presents a higher free energy at 310 K, which is now 75 meV per molecule higher in energy than our model, shown in Fig. 3. The difference in free energy is coincidental to that for free-standing layers, 76 meV, suggesting that the SA structure at RT is dominated by intermolecular H-bonds, rather than the molecule-substrate bonds as in the case at 0 K. At absolute zero the *unsaturated* HT model has stronger interaction with the substrate compared to our *saturated* structure. Thermal fluctuations weaken glycinate-Cu bonds, and free glycinate adjust themselves to maximize HB interactions while maintaining glycine-Cu interaction in a similar strength.

In fact, besides the molecule-molecule and molecule-surface interactions, the temperature plays as the third important parameter in molecular self-assembly at surfaces [4]. During the SA process, molecules interact with each other sufficiently with the help of thermal energy. In experimental conditions (temperature \sim 370 K [15] and \sim 430 K [12]), glycinate molecules move around on Cu surface in translational and rotational modes, and interact with each other by HB. The HB would break and

re-bond, providing sufficient opportunities for molecules to search for stronger intermolecular interactions. This process, together with strong polarity compensation of glycinate, promotes formation of anti-parallel HB network on Cu(001). Once formed, the structure is trapped as a metastable phase even at very low temperatures. The fact that the structure we proposed is observed at a temperature as low as 5 K in experiments, implies that transition from our structure to the “ground-state” HT structure could be blocked by a large energy barrier. We emphasize that the SA structure at a finite temperature is determined by the free energy, rather than the total energy at 0 K. The molecule-surface interaction decides the adsorbed glycinate molecular configuration in the tridentate fashion, but the intermolecular interaction plays a dominant role for the glycinate SA arrangements on Cu(001). Therefore, it is demonstrated that at finite temperature the SA on surfaces are mainly determined by the relatively weak HB rather than the stronger interfacial interaction.

Based on above investigations, we summarize a general rule for the construction of glycinate SA structures on Cu surface. The rule has three elementary components: (i) Because of the strong polarity, the positive site of a glycinate interacts with the negative site of another via hydrogen bond to form a head-to-tail chain. (ii) The polarity of glycinate also affects its side neighbors, i.e., the positive sites of neighbors will approach to the negative site of the glycinate, and vice versa. Thus, (i) and (ii) together result in the *local* molecular configurations where the positive site of each glycinate is surrounded by the three neighbors’ negative sites, and the negative site surrounded by the three positive sites. (iii) Each glycinate molecule contributes its all active sites, *two positive sites* in amino group and *two negative sites* in carboxyl group, to interact with its neighbors via HB. According to the rule (iii), glycinate molecule will automatically adjust its chirality, an important feature associated with SA, to self-organize HB network structures. These three principles for constructing glycinate SA are collectively called the polarity compensation rule here.

Besides the dominant heterochiral $p(2 \times 4)$ phases widely observed in experiments [12, 15], homochiral phases were also found by several groups for glycinate SA on Cu(001) [12, 16]. The presence of both heterochiral and homochiral phases induces a variety of SA patterns in STM images [16], e.g. a homochiral array at the boundary between heterochiral $p(2 \times 4)$ phases. To reach a unified understanding on these rich SA patterns, we invoke the polarity compensation rule to unravel the underlying mechanism for the formation of different chiral phases.

We first look at the boundary between two $p(2 \times 4)$ domains, $p_1(2 \times 4)$ and $p_2(2 \times 4)$, where p_2 is shifted by one lattice of Cu surface along $[\bar{1}10]$ with respect to p_1 , shown in Fig. 4. At the boundary, the glycinate with

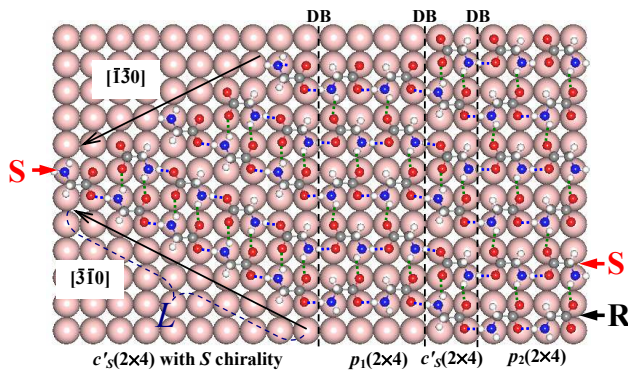


FIG. 4: Molecular arrangements for comparing with STM images in Ref. [16], where exhibit various structures including the heterochiral $p(2 \times 4)$ and homochiral $c'_S(2 \times 4)$ domains and their relationship. Dashed lines indicate domain boundaries.

R chirality has to turn its head into S chirality in order to form a strong HB across the boundary and a weak HB with the side neighbor. Thus all molecules at the leftmost column of $p_2(2 \times 4)$ become S chirality, denoted as $p'_S(2 \times 4)$ in Fig. 4. This homochiral glycinate array must exist between the shifted heterochiral p_1 and p_2 domains, offering full HBs to stabilize the boundary and lowering the energy by ~ 100 meV per molecule. This simple mechanism provides a natural explanation for the well observed homochiral phase between $p(2 \times 4)$ domains in experiment, indicated by white arrows in Fig. 2(e) of Ref. [16].

The above observation demonstrates how glycinate changes its chirality to interact with its neighbors according to the rule when the molecule shifts along $[\bar{1}10]$ by a Cu position. Shifting continuously in this way, all glycinate with R chirality would change to S chirality in order to bond together, so a complete homochiral phase of S chirality is formed. More importantly, this homochiral phase naturally develops a step along the $[\bar{3}10]$ direction, on which all molecules are saturated with HB and the step becomes inactive, shown in the left corner of Fig. 4 and Fig. 5. This triangular $p'_S(2 \times 4)$ phase is indeed observed by STM, denoted as $c(2 \times 4)$ in Fig. 2(e) of Ref. [16].

Since glycinate is enantiomeric, it is expected that an alternative homochiral $c'_R(2 \times 4)$ phase with all R chirality also exists. Indeed this homochiral R -phase is formed in the same way at the right side of the $p(2 \times 4)$ pattern, illustrated in Fig. 5. Similarly, this phase could also be formed by shifting the glycinate molecules along $[\bar{1}10]$ at the left side of the $p(2 \times 4)$ pattern by a Cu position, while the $c'_S(2 \times 4)$ phase at the right side. Both c'_S and c'_R phases are composed of hydrogen-bonded twin chains. Besides the aforementioned homochiral phases, by shifting the glycinate a Cu position along $[110]$ sequentially, other two homochiral phases above and below

the $p(2 \times 4)$ pattern can also be constructed based on our rule, named as $c_S(2 \times 4)$ and $c_R(2 \times 4)$ in the upper and lower part of Fig. 5, respectively. The chirality of the outermost glycinate in the $p(2 \times 4)$ phase decides the chirality of the c phase. Since each adsorbed glycinate molecule occupies a (2×2) Cu surface cell, every possibility for the c' and c phases by shifting a Cu position along each direction has been considered. It should be noted that all above homochiral phases are different from the $c(2 \times 4)$ phase model adopted by Kanazawa et al.[16].

We have exhausted all possible SA structures of glycinate on Cu(001): a unique heterochiral $p(2 \times 4)$ phase and four homochiral phases based on our rule. In particular, the chirality of each phase is automatically determined by the rule (iii). The interrelationships between various phases are displayed in Fig. 5 where the heterochiral $p(2 \times 4)$ phase is surrounded by different homochiral phase in each direction. The reason that we put them together is to emphasize their *seamless* connections where the boundaries between the hetero- and homo-chiral phases also obey our rule. No matter where a glycinate molecule locates in single phase or boundary, it fully interacts with the neighbors by two positive sites in amino group and two negative sites in carboxyl group via HB without any exception. To our knowledge, glycine on Cu(001) exhibits the richest 2D SA structures on surface, in which all SA patterns and their interrelationships are naturally explained under a single mechanism. Since $p(2 \times 4)$ and $c'_S(2 \times 4)$ structures have already been observed in STM experiment[16], searching for other predicted phases experimentally remains a challenge to prove our theory.

To conclude, we have clarified that the self-assembly structure is determined by the free energy at finite temperature, and revealed the mechanism for self-assembly of glycine on Cu(001) based on full polarity compensation. The ideality of H bonding environment reaches a unique antiparallel head-to-tail network of glycinate in $p(2 \times 4)$ phase. We elucidate that thermal fluctuations at finite temperatures weaken the molecule-substrate interaction and favor the intermolecular interactions, which plays a dominant role to orchestrate glycine self-assembly. The long-term controversy about competing phases, i.e., homechiral phase and heterochiral phase, as well as their relationships has been uniformly resolved in the same framework. The present work represents a distinct example that self assembly of molecules is driven by intermolecular interactions themselves, rather than being fixed by interacting with templates, even though the molecule-template interaction is stronger at 0 K. Although demonstrated for a small molecule on a simple surface, the SA mechanism and the rule revealed here are expected to have much wider implications in understanding self-assembly of polar molecules with other templates and of larger biomolecules in biologically relevant environments [4, 5].

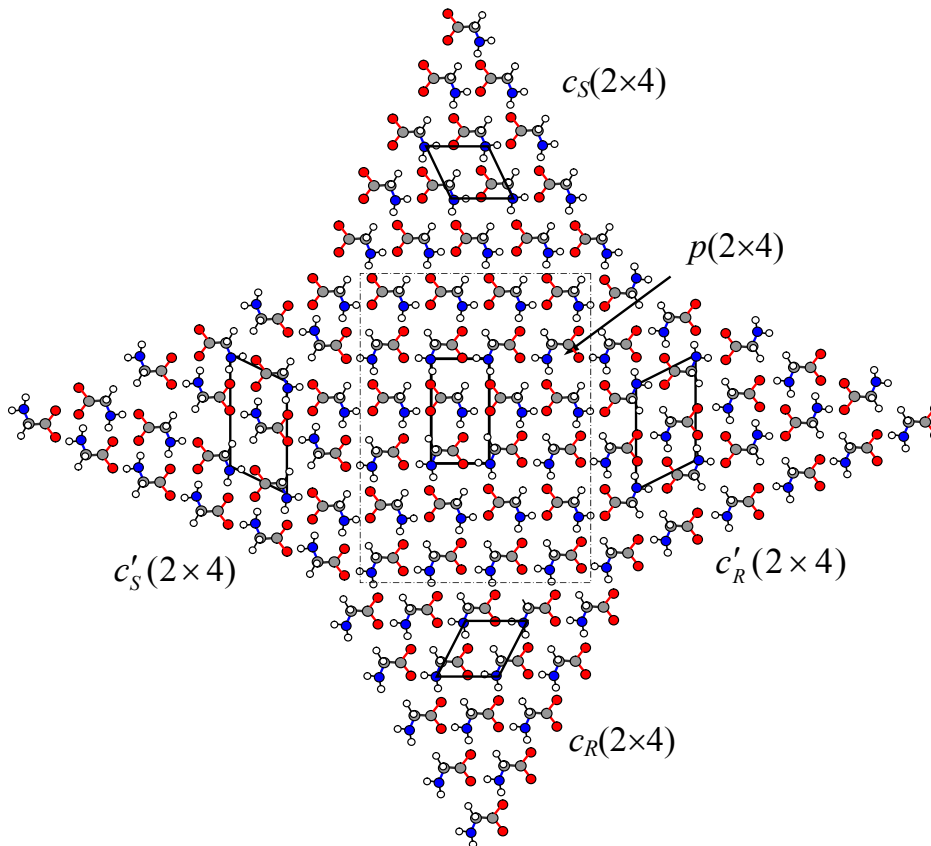


FIG. 5: Panorama of the SA monolayer of glycinate on Cu (001). There are four homochiral phases around the heterochiral phase $p(2 \times 4)$. Domain boundaries are represented by the dashed lines, and the unit cell for each phase is denoted by solid lines. For the sake of clarity, the Cu substrate is not shown.

* Electronic address: lfxu@iphy.aphy.ac.cn.

- [1] J. V. Barth, G. Costantini, and K. Kern, Nature (London) **437**, 671 (2005).
- [2] F. Höök et al., ACS Nano 2008, **2**, 2428-2346.
- [3] M. Böhringer et al., Phys. Rev. Lett. **83**, 324 (1999).
- [4] J. V. Barth et al., Angew. Chem. Int. Ed. **39**, 1230 (2000).
- [5] J. Weckesser et al., Phys. Rev. Lett. **87**, 096101 (2001).
- [6] A. Kühnle et al., Phys. Rev. Lett. **93**, 086101 (2004).
- [7] T. Yokoyama et al., Nature **413**, 619-621 (2001).
- [8] S. Stepanow et al., Nat. Mat. **3**, 229-233 (2004).
- [9] J. A. Theobald et al., Nature **424**, 1029-1031 (2003).
- [10] R. Madueno et al., Nature **454**, 618-621 (2008).
- [11] G. Pawin et al., Science **313**, 961-962 (2006).
- [12] (a) X. Zhao, et al., Surf. Sci. **424**, L347-L351 (1999); (b) X. Zhao, et al., Mater. Sci. Eng. C **16**, 41-50 (2001).
- [13] V. Efstathiou and D. P. Woodruff, Surf. Sci. **531**, 304 (2003).
- [14] P. Messina et al., J. Am. Chem. Soc. **124**, 14000-14001 (2002).
- [15] K. Kanazawa et al., J. Am. Chem. Soc. **129**, 740-741(2007).
- [16] K. Kanazawa et al., Phys. Rev. Lett. **99**, 216102 (2007).
- [17] M. S. Dyer and M. Persson, J. Phys.: Condens. Matter **20**, 312002 (2008)
- [18] Z. X. Hu, W. Ji and H. Guo, Phys. Rev. B **84**, 085414 (2011).
- [19] G. Kresse and J. Hafner, Phys. Rev. B **47**, 558 (1993).
- [20] G. Kresse and J. Furthmüller, Phys. Rev. B **54**, 11169 (1996)
- [21] Y. Wang and J. P. Perdew, Phys. Rev. B **44**, 13298 (1991).
- [22] H. J. Monkhorst and J. D. Pack, Phys. Rev. B **13**, 5188 (1976).
- [23] S. Meng et al., Phys. Rev. Lett. **89**, 176104 (2002).
- [24] J. J. Yang et al., Phys. Rev. Lett. **92**, 146102 (2004).
- [25] J. Tersoff and D. R. Hamann, Phys. Rev. B **31**, 805 (1985).
- [26] K. Mae and Y. Morikawa, Surf. Sci. **553**, L63 (2004).